OUTPHASING ELEMENTS FOR HYBRID ANALOGUE DIGITAL BEAMFORMING AND SINGLE-RF MIMO

Bernhard Gäde[⋆] *Michael Amon*[†] *Ali Bereyhi*[⋆] *Georg Fischer*[†] *Ralf R. Müller*[⋆]

[⋆]Institute for Digital Communications, [†]Institute for Electronics Engineering,
Friedrich-Alexander-University Erlangen-Nuremberg, Germany

ABSTRACT

In conventional Multiple-Input Multiple Output (MIMO) systems, each antenna requires its own Radio Frequency (RF) chain. Since each RF-chain includes several active components that have to be synchronised, costs and complexity become restrictive. The outphasing MIMO and the outphasing precoder architectures are possible approaches to mitigate this problem. The core of both architectures are Outphasing Elements (OEs), which are used to form a electronically controllable, passive antenna feed network. In this paper, these OEs are analysed with respect to component tolerances. The feasibility of the outphasing concept is demonstrated by the implementation of a hardware prototype OE. The performance of this prototype is measured and compared to theoretical predictions with good agreement.

***Index Terms*—** Massive MIMO, Single-RF, Outphasing

1. INTRODUCTION

Massive MIMO will be almost surely included in the upcoming 5G mobile communications standard. However, despite the theory behind massive MIMO is well understood and mature these days, sustainable concepts for hardware architectures lag behind. In a naive approach, conventional transceivers are simply scaled up to support a large number of antennas. In this case, an RF-chain is allocated to every antenna. Each RF-chain includes several active components, such as Power Amplifiers (PAs), mixers, Analogue-to-Digital, and Digital-to-Analogue Converters (ADCs/DACs). The requirement of high speeds of the converters as well as linearity of the PAs makes these components the most power-consuming and cost-dominating elements in the RF block of a transceiver. As a result, in a conventional architecture, power consumption and hardware costs scale linearly with the number of antennas. In mobile networks with ordinary user equipment, power consumption and production costs are always critical, even in less massive MIMO settings.

In the context of massive MIMO systems, several approaches have been proposed in order to overcome this complexity-cost issue. Primary approaches, such as antenna selection, try to address this challenge by some pre-processing techniques while using the conventional transceiver structures [1, 2]. On the other hand, recent approaches, such as Hybrid Analogue Digital Beamforming (HADB) propose new transceiver architectures which, along with signal processing techniques, improve the overall efficiency of the system [3, 4]. In HADB, the number of antennas is reduced to the number of data streams to be supported. In the baseband stage, this structure allows for standard digital signal processing. The low-dimensional channel seen by the digital precoder is moreover enhanced via analogue beamforming. Various analogue beamformers have been proposed in literature, most of which suffer from large signal-dependent losses or are restricted to phase weights [5]. This issue has been addressed in a recent application of OEs, known as Outphasing Precoder Architecture (OPA), which provides amplitude and phase control without dynamic losses [6].

1.1. Single-RF architectures

Single-RF MIMO refers to a transceiver structure where all antennas are fed by a single RF-chain. The electronically steerable passive radiator is a single-RF architecture where an active antenna element is closely surrounded by a number of passive antenna elements. The latter are connected to electronically tunable passive reactances. Altering these reactances results in a variation of the overall antenna array pattern. This fact is exploited for beamforming and spatial multiplexing [7]. However, since strong coupling among the antennas is required, the maximum number of antennas and the degrees of freedom are limited.

Load Modulated MIMO (LMM) has been proposed as a more flexible single-RF architecture. In this architecture, all antenna branches are connected to a single PA. Each antenna current is controlled by a lossless two-port network connected in series with the respective antenna [8]. The design of this architecture confronts with two major challenges. First, a common star point of constant RF voltage is required, from which all antenna branches emerge. The implementation of such a star point is very challenging as it has to connect a multitude of transmission lines without being electrically large. Second, the transmission lines from the star point to the load modulators are inherently unmatched which can cause losses

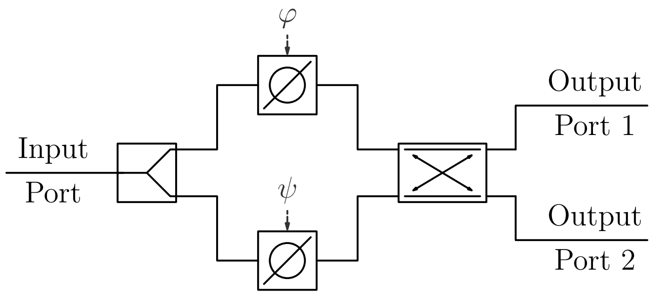

Fig. 1. Block diagram of an OE.

and distortions due to reflections. Using OEs, the star point can be replaced by a power distribution tree. This structure is referenced as OMA. It is shown, that this structure is in theory lossless and matched while supporting the same modulation schemes as LMM [9].

1.2. Contributions

In this study, we present the detailed design as well as the experimental results of the first OE hardware prototype. To this end, we first give a brief introduction to the main applications of OEs in Section 2, namely the OPA and OMA architectures. A sensitivity analysis of OEs with respect to (w.r.t.) component tolerances is discussed in Section 3. The results give guidelines in selecting suitable components and show certain limitations of OEs. The measurement results of the hardware prototype are demonstrated in Section 4. The final remarks and a conclusion is given in Section 5.

2. OUTPHASING MIMO AND PRECODER ARCHITECTURES

The key problem in both HADB and LMM is to find a lossless analogue network which connects multiple antennas to a single RF-chain and allows for different amplitude and phase weights at each antenna. Using OEs, it is possible to implement a distributed power split network that is theoretically lossless and fully matched [6, 9]. As shown in Fig. 1, each OE employs a Wilkinson power divider to equally split the signal at the input port. In the subsequent switched-line phase shifters, the phases of the signal components are shifted by the angles φ and ψ, respectively. Both signals are fed into mutually isolated ports of a $90°$ hybrid coupler, such that a sum and a difference signal appear at the two output ports. The ideal *transfer functions* of a single OE from the input port to the output ports at the centre frequency read [6]:

$$f_1(\varphi,\psi) = \frac{1}{2}\left(-\mathrm{e}^{-\mathrm{j}\varphi} + \mathrm{j}\,\mathrm{e}^{-\mathrm{j}\psi}\right) \tag{1a}$$

$$f_2(\varphi,\psi) = \frac{1}{2}\left(\mathrm{j}\,\mathrm{e}^{-\mathrm{j}\varphi} - \mathrm{e}^{-\mathrm{j}\psi}\right). \tag{1b}$$

3. SENSITIVITY ANALYSIS OF OES

In OMA and OPA with N antennas per feed network, OEs are connected to a tree of depth $\log_2 N$. Thus, small deviations in magnitude and phase per OE can cause a large accumulated error at the antennas. As a consequence, appropriate OE component selection is required to prevent a significant performance degradation. On the other hand, increasing the costs by unnecessarily choosing overspecified components should be avoided as well. This is achieved by investigating the impact of component tolerances on the OE operation.

To start with the analysis, let $f_p(\varphi,\psi,\boldsymbol{x})$ be the transfer function of a nonideal OE to the output port $p \in \{1,2\}$. Here, φ and ψ denote the phase shifts and the vector $\boldsymbol{x}$ represents the nonidealities, namely: unequal insertion losses of the phase shifters, deviations from the $3\,\mathrm{dB}$-coupling coefficients of the Wilkinson divider and the hybrid coupler, and mismatched delay lines of the phase shifters. To assess the sensitivity w.r.t. these parameters, the one-at-a-time partial derivative approach is chosen. The simplicity of this approach allows for clear analytical results which reveal the most critical components and specifications. In contrast to other methods, no detailed information about the uncertainty of the individual parameters is required, which is often unavailable in datasheets [10].

Since the transfer function of an OE is complex-valued, the sensitivity coefficients are separately calculated for magnitude and phase as follows:

$$s_{\mathrm{mag},x_\mathrm{i},p}(\varphi,\psi) = \left.\frac{\partial\,|f_p(\varphi,\psi,\boldsymbol{x})|}{\partial x_i}\right|_{\boldsymbol{x}=\boldsymbol{0}} \tag{2a}$$

$$s_{\mathrm{arg},x_i,p}(\varphi,\psi) = \left.\frac{\partial \arg\left(f_p(\varphi,\psi,\boldsymbol{x})\right)}{\partial x_i}\right|_{\boldsymbol{x}=\boldsymbol{0}} \tag{2b}$$

Here, $s_{\mathrm{mag},x_\mathrm{i},p}(\varphi,\psi)$ and $s_{\mathrm{arg},x_\mathrm{i},p}(\varphi,\psi)$ are the magnitude and phase sensitivity coefficients of the transfer function to port p w.r.t. deviations in nonideality x_i. Note that although the partial derivatives are evaluated at $\boldsymbol{x}=\boldsymbol{0}$, i.e. for ideal parameters, they may still depend on φ and ψ. In the sequel, we derive the sensitivity coefficients for each of the nonidealities. For sake of brevity, only results for output port 1 are shown and the index p is dropped in the remainder of this manuscript. However, all results are easily extended to port 2.

3.1. Unequal insertion losses of the phase shifters

In switched-line phase shifters, different phase shifts require different transmission line lengths. These transmission lines are lossy in practice and the losses of both phase shifters in an OE are in general different. Moreover, the insertion losses of the RF switches may differ from one device to another. Any attenuation component that is equal in both phase shifters only adds a constant insertion loss to the OE without further influencing its functionality. Therefore, the analysis is restricted to a purely asymmetric attenuation nonideality where the upper

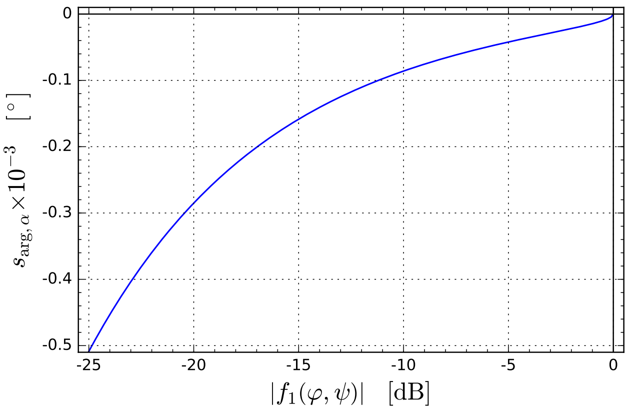

Fig. 2. Phase sensitivity w.r.t. α against magnitude.

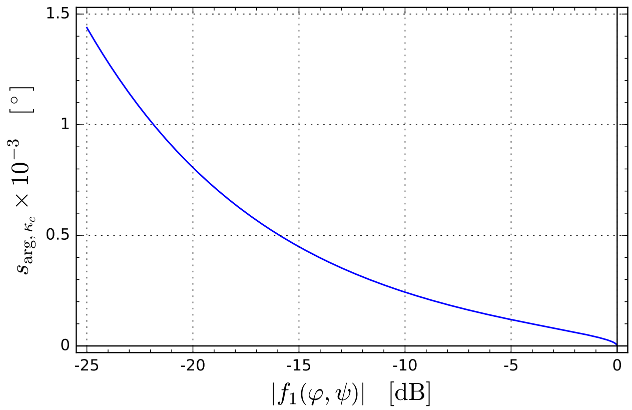

Fig. 3. Phase sensitivity w.r.t. κ_c against magnitude.

phase shifter in Fig. 1 remains ideal and the scattering matrix of the lower phase shifter is modified as:

$$\mathbf{S}_{\mathrm{ps}} = \begin{pmatrix} 0 & (1-\alpha)\,\mathrm{e}^{-\mathrm{j}\psi} \\ (1-\alpha)\,\mathrm{e}^{-\mathrm{j}\psi} & 0 \end{pmatrix} . \tag{3}$$

Here, α is the real, positive attenuation coefficient. The OE transfer function with asymmetric phase shifter insertion loss is given in Eq. (4), ignoring the influence of other nonidealities.

$$f\,(\varphi,\psi,\alpha) = \frac{1}{2}\left(\mathrm{j}\,\mathrm{e}^{-\mathrm{j}\psi} - (1-\alpha)\mathrm{e}^{-\mathrm{j}\varphi}\right) \tag{4}$$

By taking partial derivatives of magnitude and phase of Eq. (4) w.r.t. α, the sensitivity coefficients are given as:

$$s_{\mathrm{mag},\alpha} = -\frac{\sin(\varphi-\psi)+1}{2\sqrt{2\,\sin(\varphi-\psi)+2}} \tag{5a}$$

$$s_{\arg,\alpha} = -\frac{\cos(\varphi-\psi)}{2\,(\sin(\varphi-\psi)+1)} \tag{5b}$$

where we drop the function arguments of $s_{\mathrm{mag},\alpha}$ and $s_{\arg,\alpha}$ for readability. It can be easily verified that the magnitude sensitivity $s_{\mathrm{mag},\alpha}$ reaches its maximum value of -0.5 when $|f_1(\varphi,\psi)|$ is maximised. Note that the maximum sensitivity w.r.t. to a common attenuation in both phase shifters is unity. In the case of unequal losses only one out of two phase shifters is attenuated and consequently the maximum sensitivity is halved. The phase sensitivity $s_{\arg,\alpha}$ obviously shows a pole at integer multiples of $\varphi - \psi = -90°$. This is natural, as the magnitude is zero at these points and the phase is thus undefined. In order to understand the behaviour of the phase sensitivity also at larger amplitudes, $s_{\arg,\alpha}$, scaled by a factor of 10^{-3}, is plotted against the magnitude $|f_1(\varphi,\psi)|$ in Fig. 2. As the figure shows, the sensitivity is high also at non-vanishing magnitudes. For example, at $-20\,\mathrm{dB}$ magnitude, the sensitivity reads approximately $-285°$. In this case, for a difference in insertion losses of $0.5\,\mathrm{dB}$, i.e. $\alpha \approx 56 \times 10^{-3}$, a linear approximation of the phase error yields $E_{\arg,-20\,\mathrm{dB}} = -285° \cdot 56 \times 10^{-3} = -16°$.

3.2. Sensitivity w.r.t. nonideal coupling coefficients

In practice, hybrid couplers and Wilkinson power dividers never show a similar coupling behaviour. To model small deviations κ_{w} and κ_{h} from the optimal $-3\,\mathrm{dB}$ coupling points the scattering matrices $\mathbf{S}_{\mathrm{w}}$ and $\mathbf{S}_{\mathrm{h}}$ of the Wilkinson divider and the hybrid coupler, given in [6], are modified as follows:

$$\mathbf{S}_{\mathrm{w}} = -\mathrm{j}\begin{pmatrix} 0 & \tau_{\mathrm{w}} & k_{\mathrm{w}} \\ \tau_{\mathrm{w}} & 0 & 0 \\ k_{\mathrm{w}} & 0 & 0 \end{pmatrix} , \tag{6}$$

$$\mathbf{S}_{\mathrm{h}} = -\mathrm{j}\begin{pmatrix} 0 & \tau_{\mathrm{h}} & -\mathrm{j}\,k_{\mathrm{h}} & 0 \\ \tau_{\mathrm{h}} & 0 & 0 & -\mathrm{j}\,k_{\mathrm{h}} \\ -\mathrm{j}\,k_{\mathrm{h}} & 0 & 0 & \tau_{\mathrm{h}} \\ 0 & -\mathrm{j}\,k_{\mathrm{h}} & \tau_{\mathrm{h}} & 0 \end{pmatrix} , \tag{7}$$

where $\tau_c = \sqrt{2}/2 + \kappa_c$ and $k_c = (1-\tau_c^2)^{\frac{1}{2}}$ and $c = \{\mathrm{k},\mathrm{w}\}$. By similar lines of derivations as in Section 3.1, the sensitivity coefficients read:

$$s_{\mathrm{mag},\kappa_c} = 0 \tag{8a}$$

$$s_{\arg,\kappa_c} = \frac{\sqrt{2}\cos(\varphi-\psi)}{\sin(\varphi-\psi)+1} . \tag{8b}$$

Observe that the amplitude sensitivity vanishes for all φ and ψ whereas the phase sensitivity is a scaled version of (5b). The phase sensitivity coefficient is sketched in Fig. 3. The parameter that is often specified in datasheets of symmetric couplers and dividers is the so-called amplitude balance $B_{\mathrm{A,dB}}$, which measures the peak-to-peak amplitude difference at the output ports in dB and determines κ as $\frac{\sqrt{2}}{2}\left(10^{B_{\mathrm{A,dB}}/20} - 1\right)$. For a typical value of $B_{\mathrm{A,dB}} = 0.3\,\mathrm{dB}$, the linear error approximation at $-20\,\mathrm{dB}$ magnitude results in a phase deviation of $E_{\arg,-20\,\mathrm{dB}} = 20°$.

3.3. Mismatched phase shifter delay lines

Cost-effective Printed Circuit Board (PCB) materials, such as FR-4, are often anisotropic and poorly specified. As a result,

Table 1. Design values and measurement results for prototype OE.

	State	φ	ψ	Amplitude [dB]		Power Split [%]		Phase	
				Port 1	Port 2	Port 1	Port 2	Port 1	Port 2
Design:									
	1	90°	90°	-3	-3	50	50	45°	45°
	2	180°	90°	0	-∞	100	0	0°	–
	3	90°	120°	-0.62	-1.25	25	75	30°	30°
	4	180°	120°	-0.30	-11.7	93.3	6.7	−15°	−15°
Measurement:									
	1	–	–	-5.03	-5.07	50.2	49.8	−110.5°	−112.8°
	2	–	–	-2.13	-36.1	100	0	−156.7°	−9.7°
	3	–	–	-7.97	-3.34	25.6	49.8	−125.0°	−127.5°
	4	–	–	-2.40	-14.65	94.4	5.6	−170.4°	−171.2°

accurate matching of the transmission lines to the components is difficult, if the delay lines of the phase shifters are implemented in microstrip technology. For modelling purposes, the characteristic impedance Z_{ps} of the phase shifter transmission lines is allowed to show a small deviation ζ from the reference impedance of the system Z_{ref}, i.e. $Z_{\mathrm{ps}} = Z_{\mathrm{ref}} + \zeta$. Interestingly, the magnitude and phase sensitivities are zero, independent of the number of phase shifters modified. This implies that, as outlined in Section 3.1, the larger losses of low-cost substrates are more of concern than possible mismatches.

4. OUTPHASING ELEMENT PROTOTYPE

As a prove of concept, the hardware prototype of an OE as depicted in Fig. 4, has been implemented. It operates at $2.45\,\mathrm{GHz}$ centre frequency with one-bit phase shifters for φ and ψ. Considering the above analysis, the following components are selected: The Wilkinson divider Anaren PD2328J5050S2HF with a maximum amplitude balance of $0.3\,\mathrm{dB}$ (typical: $0.1\,\mathrm{dB}$) and the hybrid coupler Anaren XC2500A-03S with a maximum amplitude balance of $0.1\,\mathrm{dB}$. These specifications are valid over a common frequency range from $2.3\,\mathrm{GHz}$ to $2.6\,\mathrm{GHz}$. Fast switching between the two delay lines of each phase shifter is enabled by the RF switches Analog Devices HMC221B with a rise/fall time of $3\,\mathrm{ns}$. The PCB material used is Rogers RO4350B. Table 1 shows the design parameters and measurement results obtained using a Rohde & Schwarz ZVB8 vector network analyser at the centre frequency. The four possible states are designed to include the two extreme cases of an equal split between both ports as well as a fully isolated port 2. The measured relative power split ratios are in good agreement with the theoretical results. An insertion loss of the OE of approximately $2\,\mathrm{dB}$ can be derived from the measured absolute magnitudes. It is worth to indicate that the magnitude at port 2 in state 2 is not measured zero but $-36\,\mathrm{dB}$. Nevertheless it exceeds the minimum specified isolation of the coupler. Due to the non-zero length of the feed lines, the measured phases include an offset. For calculating the maximum error between the design and measurement values, all measurements are referenced to the value -156.7° measured at the first port in state 2. In this respect, absolute values of the errors do not exceed 2°, except for the measurement at the second port in state 2, where it is about $\approx 147°$. This, however, is expected as according to Section 3.1 phase sensitivities become extremely large for very low magnitudes. Since the losses of the transmission lines are very small due to the high-quality PCB substrate, the dominant source of error is expected to be nonideal coupling. Evaluating the phase sensitivity w.r.t. a nonideal coupling coefficient at the magnitude of $-11.7\,\mathrm{dB}$ and $B_{\mathrm{A,dB}} = 0.1\,\mathrm{dB}$ yields a linear error approximation of 2.5°. The measurement results suggest that, despite its simplicity, the chosen approach to sensitivity analysis gives a good basis for component selection.

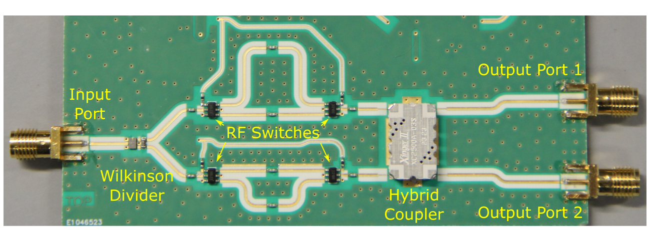

Fig. 4. PCB photograph of prototype OE.

5. CONCLUSION

The sensitivity analysis of OEs for OMA and OPA w.r.t. component tolerances depicted that the magnitude at the output ports is sufficiently robust against typical nonidealities whereas the phase shows strong sensitivity w.r.t. unequal phase shifter insertion losses and nonideal coupling coefficients. The implemented OE hardware prototype has shown close consistency with the derivations. It is hence concluded that while using OEs in OMA or OPA the architectures should provide means to calibrate the phases of the signals at the antenna ports.

6. REFERENCES

[1] A. Ghrayeb and T. M. Duman, "Performance analysis of mimo systems with antenna selection over quasi-static fading channels," *IEEE Transactions on Vehicular Technology*, vol. 52, no. 2, pp. 281–288, March 2003.

[2] Ali Bereyhi, Mohammad Ali Sedaghat, Saba Asaad, and Ralf R Müller, "Nonlinear precoders for massive mimo systems with general constraints," in *WSA 2017; 21nd International ITG Workshop on Smart Antennas*. VDE, 2017.

[3] A. F. Molisch, V. V. Ratnam, S. Han, Z. Li, S. L. H. Nguyen, L. Li, and K. Haneda, "Hybrid Beamforming for Massive MIMO: A Survey," *IEEE Communications Magazine*, vol. 55, no. 9, pp. 134–141, 2017.

[4] Thomas Kuehne and Giuseppe Caire, "An analog module for hybrid massive mimo testbeds demonstrating beam alignment algorithms," in *WSA 2018; 22nd International ITG Workshop on Smart Antennas*. VDE, 2018.

[5] Adrian Garcia-Rodriguez, Vijay Venkateswaran, Pawel Rulikowski, and Christos Masouros, "Hybrid analog–digital precoding revisited under realistic rf modeling," *IEEE Wireless Communications Letters*, vol. 5, no. 5, pp. 528–531, 2016.

[6] Bernhard Gäde, Mohammad A Sedaghat, and Ralf R Mueller, "Hybrid Analogue Digital Outphasing Beamforming Architecture with Amplitude and Phase Control," in *WSA 2018; 22nd International ITG Workshop on Smart Antennas*. VDE, 2018.

[7] Antonis Kalis, Athanasios G Kanatas, and Constantinos B. Papadias, Eds., *Parasitic Antenna Arrays for Wireless MIMO Systems*, Springer, 2013.

[8] M. A. Sedaghat, R. R. Müller, and G. Fischer, "A Novel Single-RF Transmitter for Massive MIMO," in *WSA 2014; 18th International ITG Workshop on Smart Antennas*. VDE, 2014.

[9] Bernhard Gäde, Mohammad Ali Sedaghat, Christoph Rachinger, Georg Fischer, and Ralf Müller, "A Novel Single-RF Outphasing MIMO Architecture," in *WSA 2017; Proceedings of 21th International ITG Workshop on Smart Antennas*. VDE, 2017.

[10] Andrea Saltelli, Marco Ratto, Terry Andres, Francesca Campolongo, Jessica Cariboni, Debora Gatelli, Michaela Saisana, and Stefano Tarantola, *Global sensitivity analysis: the primer*, John Wiley & Sons, 2008.